Journal of Statistical Physics, Vol. 49, Nos. 5/6, 1987

Dynamic Percolation Transition Induced by Phase Separation: A Monte Carlo Analysis

S. Hayward,[1] Dieter W. Heermann,[1] and K. Binder[1]

Received April 17, 1987; revision received July 17, 1987

The percolation transition of geometric clusters in the three-dimensional, simple cubic, nearest neighbor Ising lattice gas model is investigated in the temperature and concentration region inside the coexistence curve. We consider "quenching experiments," where the system starts from an initially completely random configuration (corresponding to equilibrium at infinite temperature), letting the system evolve at the considered temperature according to the Kawasaki "spin-exchange" dynamics. Analyzing the distribution $n_l(t)$ of clusters of size l at time t, we find that after a time of the order of about 100 Monte Carlo steps per site a percolation transition occurs at a concentration distinctly lower than the percolation concentration of the initial random state. This dynamic percolation transition is analyzed with finite-size scaling methods. While at zero temperature, where the system settles down at a frozen-in cluster distribution and further phase separation stops, the critical exponents associated with this percolation transition are consistent with the universality class of random percolation, the critical behavior of the transient time-dependent percolation occurring at nonzero temperature possibly belongs to a different, new universality class.

KEY WORDS: Percolation; phase separation; Monte Carlo simulation; lattice gas model; finite-size scaling.

1. INTRODUCTION AND OVERVIEW OF THE BACKGROUND THEORY

When one quenches a system that initially is *homogeneous on a macroscopic scale* to a state inside the "binodal" (coexistence curve), i.e., the boundary of a two-phase coexistence region, the initial homogeneous state is ther-

[1] Institut für Physik, Johannes-Gutenberg-Universität Mainz, D-6500 Mainz, Federal Republic of Germany.

0022-4715/87/1200-1053$05.00/0

822/49/5-6-12

modynamically unstable. As the time t after the quench elapses, *microscopic* inhomogeneities, which either have been present in the initial state or have been formed after the quench by statistical fluctuations, get magnified. The scale of these inhomogeneities grows and grows with time up to the *final equilibrium state*, which is *inhomogeneous on a macroscopic scale*, composed of regions of the two coexisting phases (the volume fractions of these phases are given by the lever rule).

It is commonly accepted that this spontaneous growth of inhomogeneous structures out of an initially homogeneous system may proceed by various rather distinct mechanisms, depending on whether the considered state is close to the binodal or deep inside in the two-phase region.[1-3] The decay of states close enough to the coexistence curve is believed to start by nucleation[4-6] and subsequent growth of well-isolated large-amplitude fluctuations ("heterophase fluctuations," "droplets"); these states are called "metastable." On the other hand, the decay of states well inside the two-phase region is believed to start by the growth of weak, delocalized, long-range fluctuations ("spinodal decomposition"[1-3,7-9]). These states are called "unstable states," and in mean-field-type theories metastable states and unstable states are separated by a sharp dividing line with *thermodynamically* singular behavior ("limit of metastability," spinodal curve"[7,8,10]). This line can be defined (for d less than $d^* = 6$ space dimensions[11-14]) by the condition that the free energy barrier ΔF^* against nucleation vanishes at the spinodal. It now is well accepted, however, that such a sharp spinodal line makes sense only for systems with long-range forces[14-19]; for systems with short-range forces the spinodal curve is ill-defined,[1,2,6,14,17,20] and in the kinetic mechanisms of phase separation a gradual transition from nucleation to spinodal decomposition occurs.[6,21] This transition region can only be approximately defined, e.g., by[6,10] the region from, say, $\Delta F^*_{\mathrm{MF}} = 10 k_{\mathrm{B}} T$ to $\Delta F^*_{\mathrm{MF}} = k_{\mathrm{B}} T$, where ΔF^*_{MF} is the mean-field result for the nucleation barrier; this region then always falls between the mean-field spinodal and the binodal (Fig. 1).

In the present paper, we are concerned with *different* characteristic lines in the phase diagram: we consider the *geometry of clusters defined as groups of occupied sites connected by nearest neighbor bonds.* While in the one-phase region for small c only clusters of rather small sizes occur, all clusters being well isolated from each other, with increasing c one encounters at $c_p^{(\mathrm{corr})}(T)$ a percolation transition where an infinite percolating cluster first appears, and for $c > c_p^{(\mathrm{corr})}(T)$ a finite fraction of the occupied sites belongs to the largest cluster, which hence has a size proportional to the volume of the system. The line $c_p^{(\mathrm{corr})}(T)$ ends for infinite temperature at the critical concentration of the random site percolation problem,[22-24] $c_p^{(\mathrm{corr})}(T \to \infty) = c_p^{(\mathrm{random})}$ (≈ 0.312, for the simple-cubic lattice[24,27]).

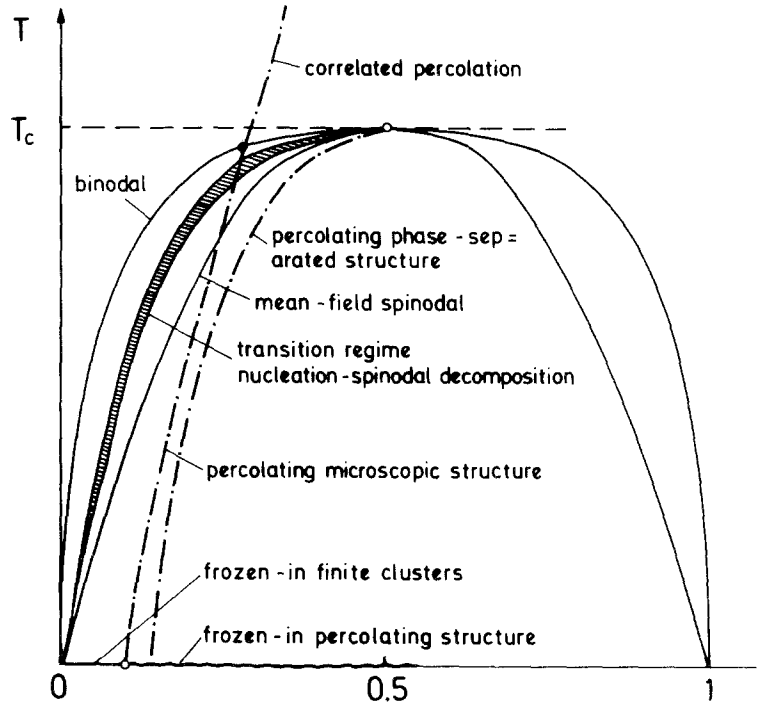

(a)

Fig. 1. (a) Schematic phase diagram of a three-dimensional, short-range lattice gas system, indicating various regions in the plane of variables temperature T versus concentration c of occupied sites, as well as various lines of percolation transitions. Since the diagram is symmetric along the line $c = 0.5$ if the meaning of occupied and empty sites is reversed, full information is given only for the regime $c \leqslant 0.5$. Shown are both the coexistence curve ("binodal") separating the one-phase region from the two-phase region and the mean-field spinodal curve separating metastable from unstable states in mean-field theory. The mean-field spinodal is described here by the equation $(0.5 - c)/0.5 = \pm(1 - T/T_c)^{1/2}$, T_c being the actual critical temperature. The transition region from nucleation to spinodal decomposition for a short-range system, as defined in the text, is also indicated. The dash-dotted curves indicate percolation transitions, as discussed in the text. Shown below are snapshots of a square lattice at $c = 0.5$ for (b) $t = 0$ and (c) $t = 40$ MCS/site, for a quench from a random initial configuration to $T/T_c = 0.5$. Occupied sites are shown by white circles (or black squares, respectively, if they belong to the largest cluster in the system), unoccupied sites are not shown. Note that the percolating cluster at $t = 40$ MCS/site has grown by aggregation of various medium-size clusters already existing at $t = 0$, which are connected together by "weak links" that form when monomers diffuse around and hit these clusters.

(b)

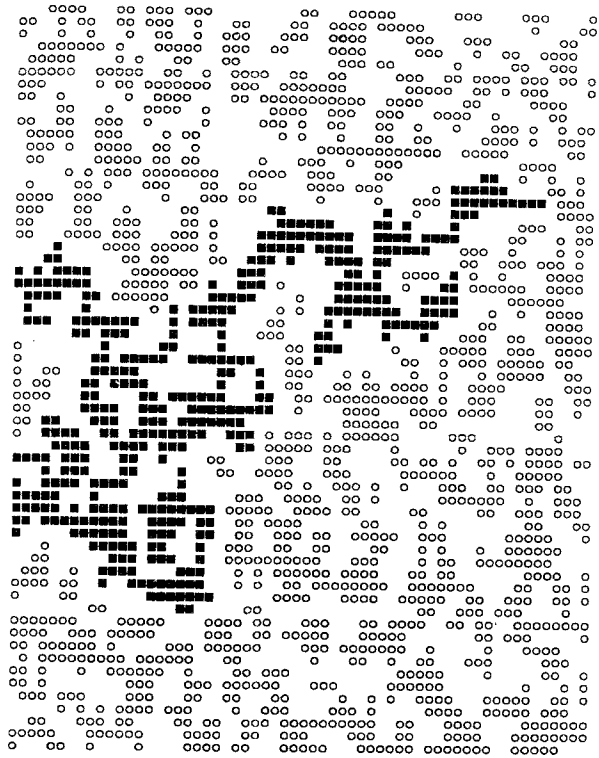

(c)

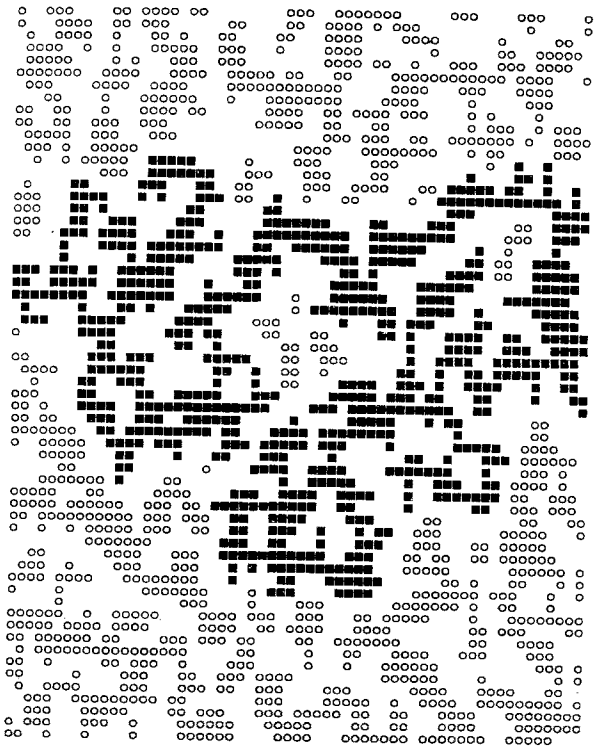

Fig. 1 (*continued*)

Although this line for $T < \infty$ describes a correlated percolation problem,[25] the correlations are of short range only and hence this percolation transition still belongs to the universality class[22] of random percolation. The line $c_p^{(\mathrm{corr})}(T)$ ends at the coexistence curve at a temperature $T \approx 0.96 T_c$[26,27].

In the present paper, we give evidence that a continuation of this line also exists inside the two-phase coexistence region, but as a *transient time-dependent phenomenon*: after short-range correlations have been built up after a time t_1, we also encounter only isolated finite clusters for $c < c_p^{(\mathrm{corr})}(T, t)$ for $t > t_1$. At a concentration $c > c_p^{(\mathrm{corr})}(T, t)$, it then happens that the system is nonpercolating for short times ($t < t_1$), and stays percolating for a finite time interval ($t_1 < t < t_2$), while later the percolating cluster has disintegrated into a set of finite clusters again.[28] The extreme case, where the infinite cluster appears only for a short time ($t_2 = t_1$), defines the so-called "dynamic spinodal" $c_p^{(\mathrm{corr})}(T, t_2 = t_1)$ in the phase diagram.[28] The other extreme case occurs for such concentrations where the system stays in a percolating state for all times exceeding t_1, i.e., when $t_2 \to \infty$, which defines another line $c_p^{(\mathrm{corr})}(T, t_2 \to \infty)$ in the phase diagram. In fact, between the lines $c_p^{(\mathrm{corr})}(T, t_2 \to \infty)$ and $c_p^{(\mathrm{corr})}(T, t_2 = t_1)$ we expect a whole family of lines, depending on the time interval $[t_1, t_2]$ being considered. In Fig. 1, we have disregarded this complication, and represent $c_p^{(\mathrm{corr})}(T, t)$ by a single line denoted "percolating microscopic structure."

It is interesting to follow the behavior of these lines down to $T = 0$. While both coexistence curve and mean-field spinodal end in the points $c = 0$, $c = 1$, the percolation line $c_p^{(\mathrm{corr})}(T, t_2 \to \infty)$ ends in a "static" percolation point $c_p^{(\mathrm{corr})}(T = 0)$ separating the regime of frozen-in finite clusters from the regime of a frozen-in percolating structure. These states are *not in equilibrium*, but are frozen in for infinite times, since at zero temperature no energy barrier can be overcome, and thus these configurations cannot relax toward the true equilibrium states (which are macroscopically separated compact regions with $c = 0$ and $c = 1$, respectively).

In addition to these percolation phenomena at a microscopic scale (where clusters are defined in terms of occupied lattice sites), at late stages of the phase separation process, where the system is phase-separated on a scale $l(t)$ into the coexisting phases with concentrations given by the two branches of the coexistence curve, $c_{\mathrm{coex}}^{(1)}$ and $c_{\mathrm{coex}}^{(2)}$, respectively, it makes sense to consider percolation phenomena on larger length scales, too. Suppose we divide our systems into cells of linear dimension l_c, with $l_c \ll l(t)$, but l_c much larger than the lattice spacing. Most of these cells will then have concentrations rather close to either $c_{\mathrm{coex}}^{(1)}$ or $c_{\mathrm{coex}}^{(2)}$. We now may define clusters consisting of neighboring cells with concentrations in a given interval $[c_{\mathrm{coex}}^{(1)} - \delta c/2, c_{\mathrm{coex}}^{(1)} + \delta c/2]$, and may ask whether these clusters are well-separated from each other or form an infinite percolating network. Since

$l(t) \to \infty$, we may then also take $l_c \to \infty$ and at the same time $\delta c \to 0$, so that there is no longer any ambiguity in this coarse-grained percolation problem. The line of this percolation transition in the macroscopic phase-separated structure must again end in the critical point; we have also included this line in Fig. 1, but do not discuss it any further in this paper. We only note that it is this line that would be experimentally accessible by techniques sensitive to the "contrast," i.e., difference in refraction index, between the two coexisting phases, such as observations by light or electron microscope. In addition, we disregard percolation phenomena that one may observe when one redefines the clusters in order that they reflect the physical correlations in the system (then the critical point is a percolation transition[29,30]). For long-range interactions, the percolation transition of these "physical clusters" coincides with the spinodal curve[12,31]; the significance of the percolation transition of "physical clusters" (in the sense of Refs. 29 and 30) inside the coexistence curve is not yet known for the case of short-range interactions, however. Previous work on percolation phenomena during phase separation either has been restricted to qualitative considerations only[32] or has studied the fractal dimension[33] of phase separation clusters at particular points in the phase diagram only.[28,34] In our opinion, the observation of fractal dimensionalities for phase separation clusters possibly can be interpreted by assuming that the data of the model of Ref. 34 were taken not very far from the line $c_p^{(\mathrm{corr})}(T, t)$. This assumption is consistent with the observation in Ref. 34 that about one-half of all the atoms did belong to the percolating cluster that was analyzed—such a value of the percolation probability occurs close to a percolation threshold only. In two dimensions cluster properties of a phase separating system on a triangular lattice have been studied[67] at a concentration $c = 1/2$. However, there the system always stays percolating.

Another question that needs to be addressed but is outside of the scope of the present work concerns the extent to which the percolation transition at $c_p^{(\mathrm{corr})}(T, t)$ has any effect on experimentally observable quantities, such as the structure factor $S(\mathbf{k}, t)$. Predicting $S(\mathbf{k}, t)$ at the later stages of phase separation is a formidable problem[1,2,9,21,35,36]; since many ideas on the subject use concepts on cluster dynamics,[21,35–37] understanding of the cluster geometry may be a useful ingredient of a more complete theory. Also, we do not analyze in any detail the time dependence of the "kinetic gelation" by which the small clusters present initially aggregate to form the infinite percolating net, for $c \geqslant c_p^{\mathrm{corr}}(t_1 = t_2)$.

In Section 2, we describe in more detail the model simulated to map out the line $c_p^{(\mathrm{corr})}(T, t)$ in Fig. 1, and explain the procedures by which the

simulation data were analyzed. Section 3 discusses critical exponents on the basis of a finite-size scaling[38–40] analysis. Section 4 contains a discussion of our results and an outlook on possible future work.

2. MONTE CARLO INVESTIGATION OF DYNAMIC PERCOLATION IN THE SIMPLE CUBIC LATTICE

We study simple cubic L^3 lattices, choosing linear dimensions $L = 10, 15, 20, 30$, and 40 (the two smallest linear dimensions have been found less useful and are included only occasionally). For $T = 0$, also $L = 50$ is considered. The initial state of each simulation run is a completely random configuration. We then let the system evolve in time using the standard Kawasaki-type[41] dynamics, as usual for Monte Carlo simulations of phase separation.[42,43],[2] In each run we monitor the time evolution of the size of the largest cluster, applying standard cluster counting and cluster identification algorithms.[45,27,28] Of course, there occur huge fluctuations in the size of the largest cluster; therefore, it is necessary for each choice of the variables temperature T, concentration c, and lattice linear dimension L to take a sample of n statistically independent time evolutions, where typically $n = 40$–50. These n different time evolutions are generated by choosing different random numbers for each random starting configuration, as well as different random numbers for executing the desired random exchanges by which the time evolution of the model proceeds.

As an example, Fig. 2a shows the time evolution of the largest cluster for $T/T_c = 0.3$ at short times (0–80 Monte Carlo steps/site) and Fig. 2b shows the results for a longer time scale (0–800 Monte Carlo steps/site). It is seen that in the short-time regime the cluster size increases rapidly with increasing time, reaches a maximum, and then decreases. It is also recognized that in spite of using a system of 64,000 lattice sites and averaging over a sample $n = 40$–50, there are still appreciable fluctuations in cluster size. In order to gain statistics we hence have averaged these "raw data" over a time interval Δt for such times where the cluster size distribution $n_l(t)$ did not change much with time. Obviously, this cannot work for the early-time regime, where $n_l(t)$ strongly increases for large l (at the expense of small clusters, in particular monomers, which are present initially but gradually disappear as phase separation proceeds). Most of the data analyzed below are averages over the interval from $t = 80$ to $t = 240$ MCS/site, i.e., the region of the peaks in Fig. 2. We have analyzed similarly the behavior in the later-time region from $t = 640$ to

[2] See also Ref. 44 for more details.

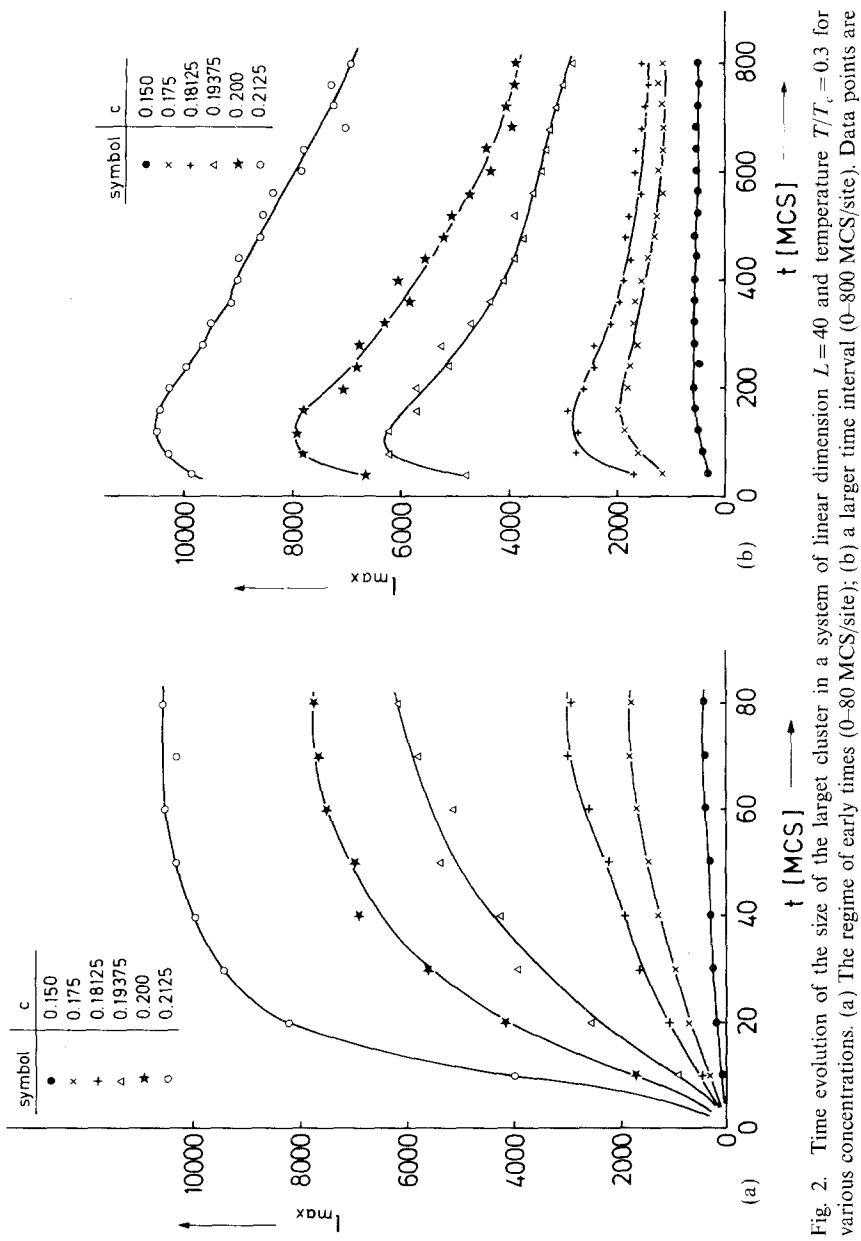

Fig. 2. Time evolution of the size of the largest cluster in a system of linear dimension $L = 40$ and temperature $T/T_c = 0.3$ for various concentrations. (a) The regime of early times (0–80 MCS/site); (b) a larger time interval (0–800 MCS/site). Data points are the result of sampling over $n = 40$–50 statistically independent time evolutions. Curves drawn are guides to the eye only.

$t = 800$ MCS/site for $T/T_c = 0.3$; the decrease of the size of the largest cluster seen in Fig. 2 leads to a slight increase of the percolation concentration $c_p^{(\mathrm{corr})}(T, t)$ with time.

If the final temperature T of the quench is $T = 0$, the behavior is somewhat different (Fig. 3). After a relatively short time, a stationary cluster size distribution is reached. This behavior is easily interpreted physically: at $T = 0$, only such exchanges are possible that do not involve any energy cost.[3] If the initial state did consist of an assembly of well-separated small clusters, as happens in the regime of concentrations far less than the percolation threshold $c_p^{(\mathrm{random})}$, basically only monomers are mobile (Fig. 4). These monomers will diffuse around until they get attached to some of the larger, immobile clusters. Although some motion is also possible for the larger clusters (Fig. 4b) and even within the infinite percolating net (Fig. 4d), such motions are not sufficient to maintain a coarsening of the structure. Due to the coarsening at nonzero temperature some loosely bound parts of the largest cluster break off again,[32] and this effect leads to a decrease of the size of the largest cluster at intermediate time scales. But even at zero temperature an analytic treatment of the "cluster dynamics" is not possible on a rigorous basis, as additional monomers may be created due to processes such as shown in Fig. 4c. Due to processes similar to those of Fig. 4b, sometimes one also reaches states where the cluster size distribution is not exactly stationary, but is irregularly oscillating in time: These fluctuations are also smoothed out by averaging over suitable time intervals Δt.

Figure 5 summarizes our results for the percolation probability P_∞, which we have estimated by dividing the number of occupied sites contained in the largest cluster by the total number of occupied sites. It is seen that there occur rather pronounced finite-size effects in the concentration regime of interest; an analysis of these finite-size effects will be attempted in the next section. Here we only note that the curves for P_∞ for different L intersect in a rather narrow concentration interval, which can be taken as an upper bound for any estimate of $c_p^{(\mathrm{corr})}(T, t)$, t being chosen in the interval Δt from $t = 80$ to 240, as noted above. Figure 6 shows a quantitative phase diagram of the simple cubic lattice gas model, including the results for $c_p^{(\mathrm{corr})}(T, t)$ resulting from Fig. 5. In order to check for any systematic errors due to the smoothing of the data over the time interval Δt, we have also analyzed data for P_∞ taken at the fixed time $t = 120$ and verified that the resulting curves within their error bars are completely indistinguishable from those shown in Fig. 5.

[3] Previous work on phase separation kinetics at $T = 0$ has been performed for concentration $c = 1/2$ only.[46]

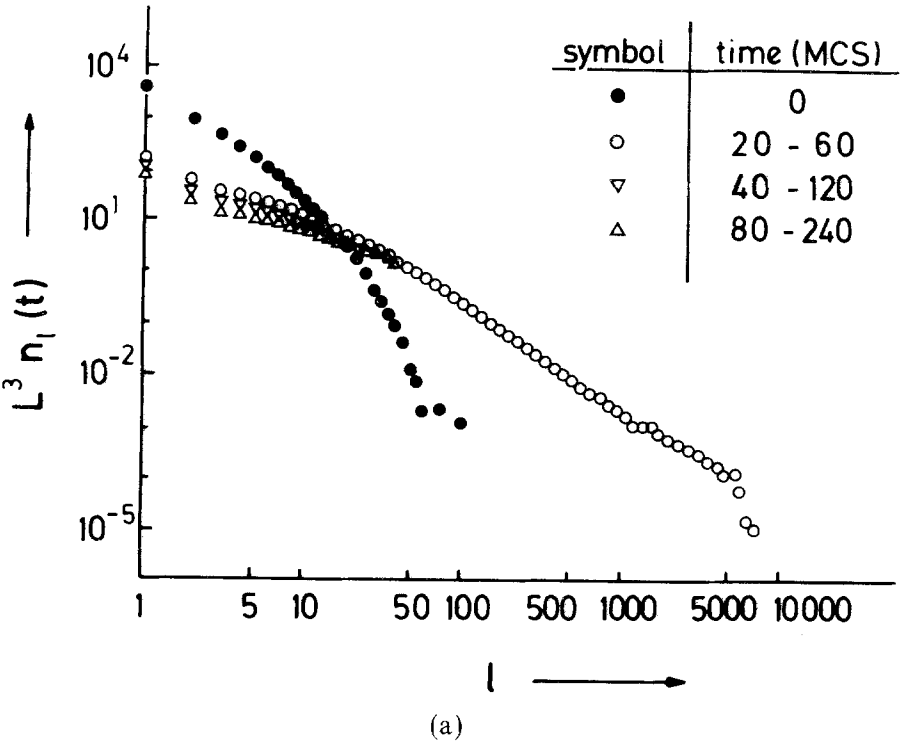

(a)

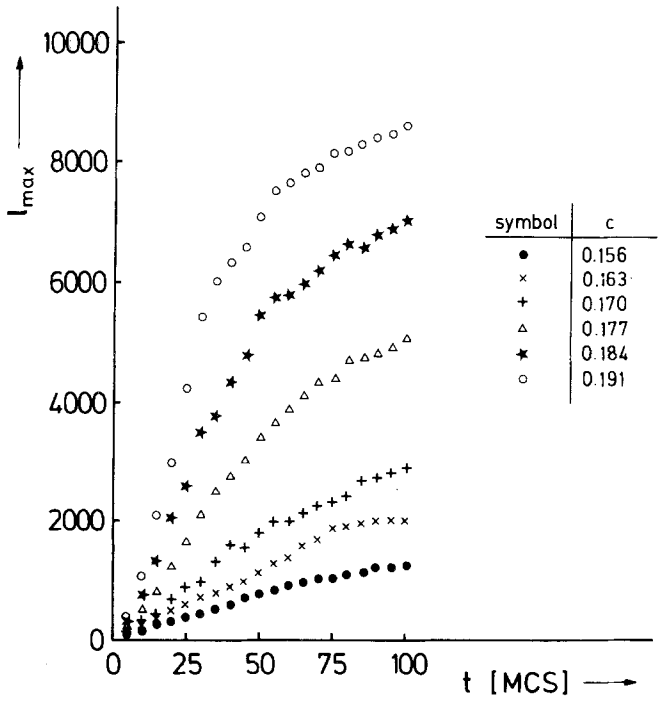

(b)

Fig. 3. Time evolution of (a) the full cluster size distribution and (b) the size of the largest cluster, in a system of linear dimension $L = 40$ and temperature $T = 0$ for concentrations and times, respectively. Data points are the result of sampling over $n = 40$–50 statistically independent time evolutions.

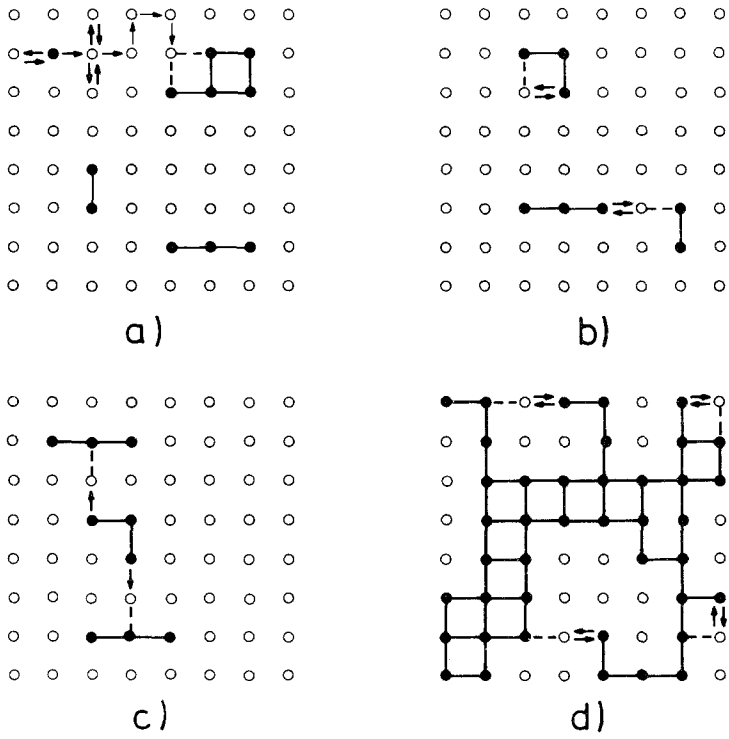

Fig. 4. Motions possible in quenching experiments at $T=0$. (a) A configuration with a monomer, indicating that after a random walk motion it gets attached to a pentamer. Hereafter the configuration is frozen. (b) A configuration containing two trimers and one dimer. Although the motions indicated in the figure can go on back and forth indefinitely, they do not affect the cluster size distribution. (c) A situation where two motions destroy a trimer and create a free monomer again. (d) Motions of dangling ends in a percolating cluster at $T=0$.

Of course, it also is of interest to compute and analyze various other quantities that characterize the cluster size distribution $n_l(t)$ near this percolation transition. For example, we are interested in the "susceptibility"[22–24]

$$\chi = \sum_{l}{}' l^2 n_l(t) \tag{1}$$

where the prime indicates that the largest cluster in the system is excluded from the summation. Figure 7 shows data for χ at $T=0$. One finds the familiar picture of a peak that grows to infinity as $L \to \infty$. Extrapolation of the peak position gives another criterion to locate the percolation concentration, as indicated in the inset.

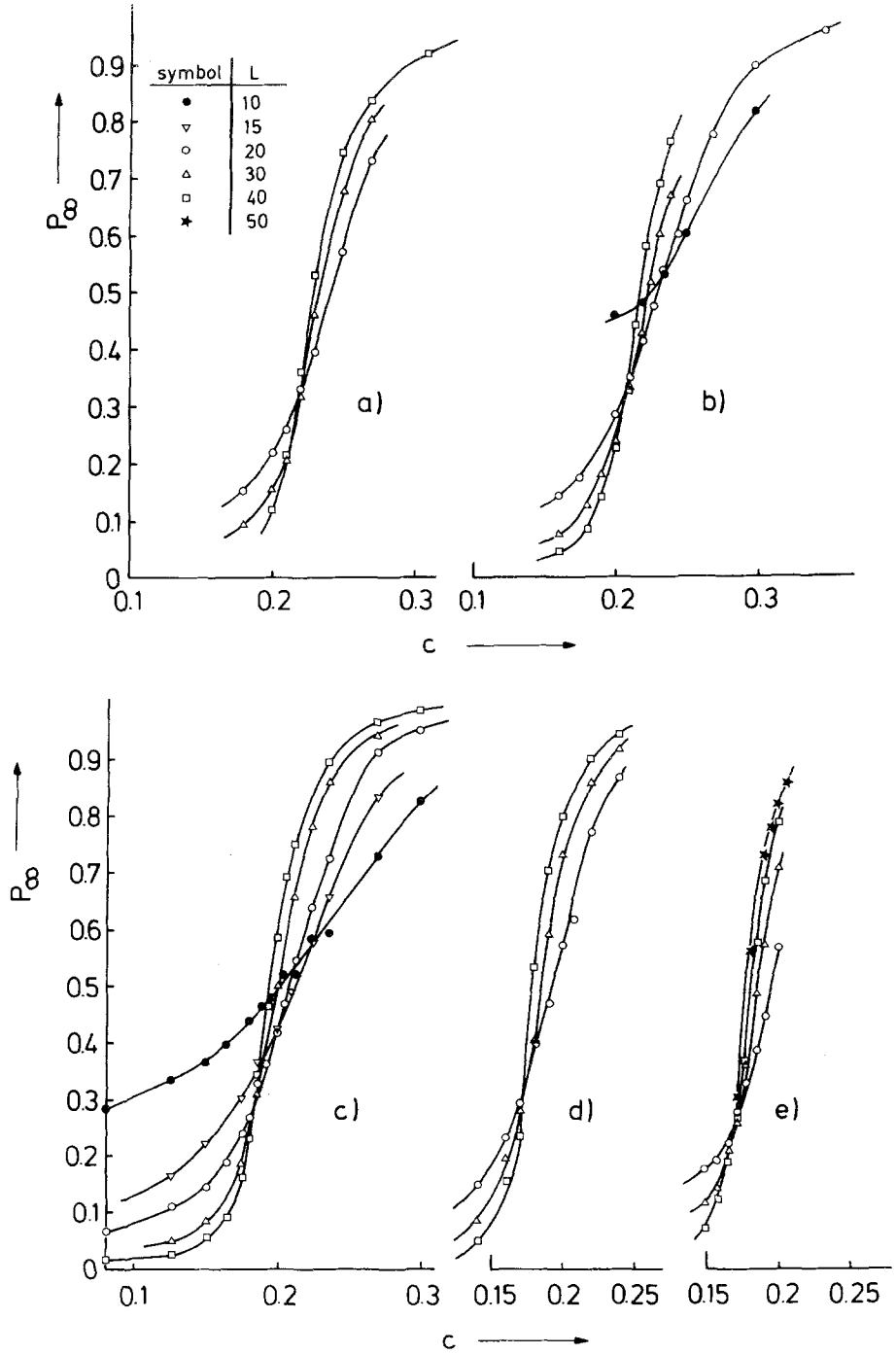

Fig. 5. Percolation probability P_∞ plotted versus concentration c in the lattice gas model, for temperatures $T/T_c =$ (a) 0.75, (b) 0.6, (c) 0.3, (d) 0.15, and (e) 0, and various values of L as indicated. Data are obtained from time averages from $t = 80$ to $t = 240$ MCS/site during phase separation, and sample averages over $n = 40$–50 runs were taken.

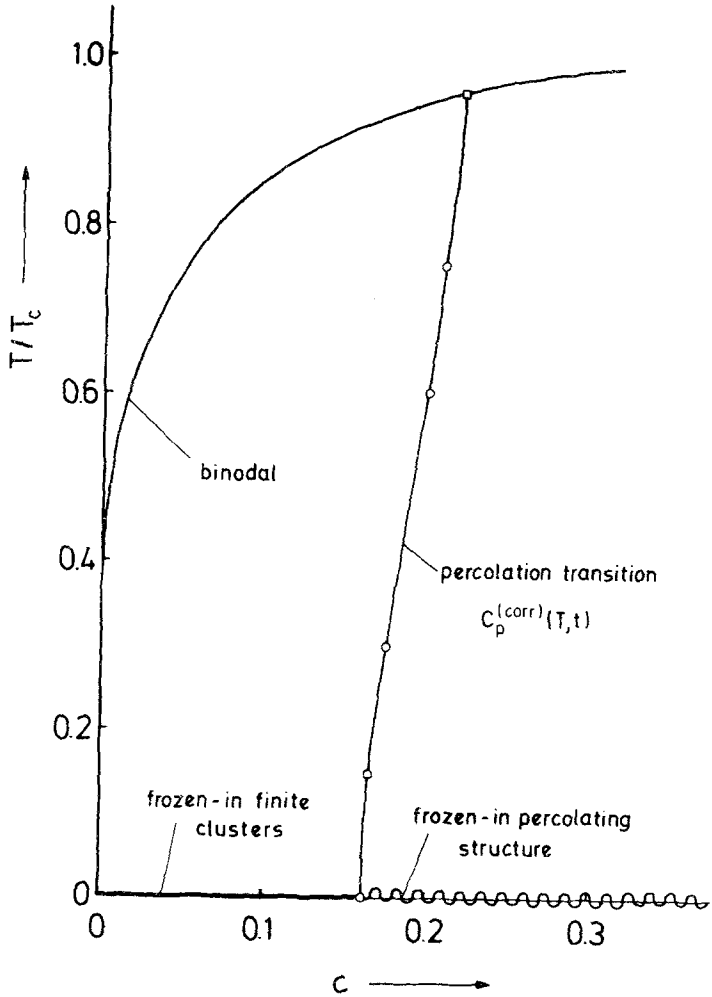

Fig. 6. Part of the phase diagram of the simple cubic, nearest neighbor lattice gas model, showing the percolation transition line as determined in the present paper. The time t refers to an average over the time interval from $t=80$ to $t=240$ MCS/site during phase separation. The error in our estimates for $c_p^{(corr)}(T, t)$ is roughly given by the size of the points. The estimate for $c_p^{corr}(T)$ at the coexistence curve is taken from Ref. 27. The estimates for $c_p^{(corr)}(T, t)$ shown here are based on the extrapolation procedure illustrated in Fig. 8.

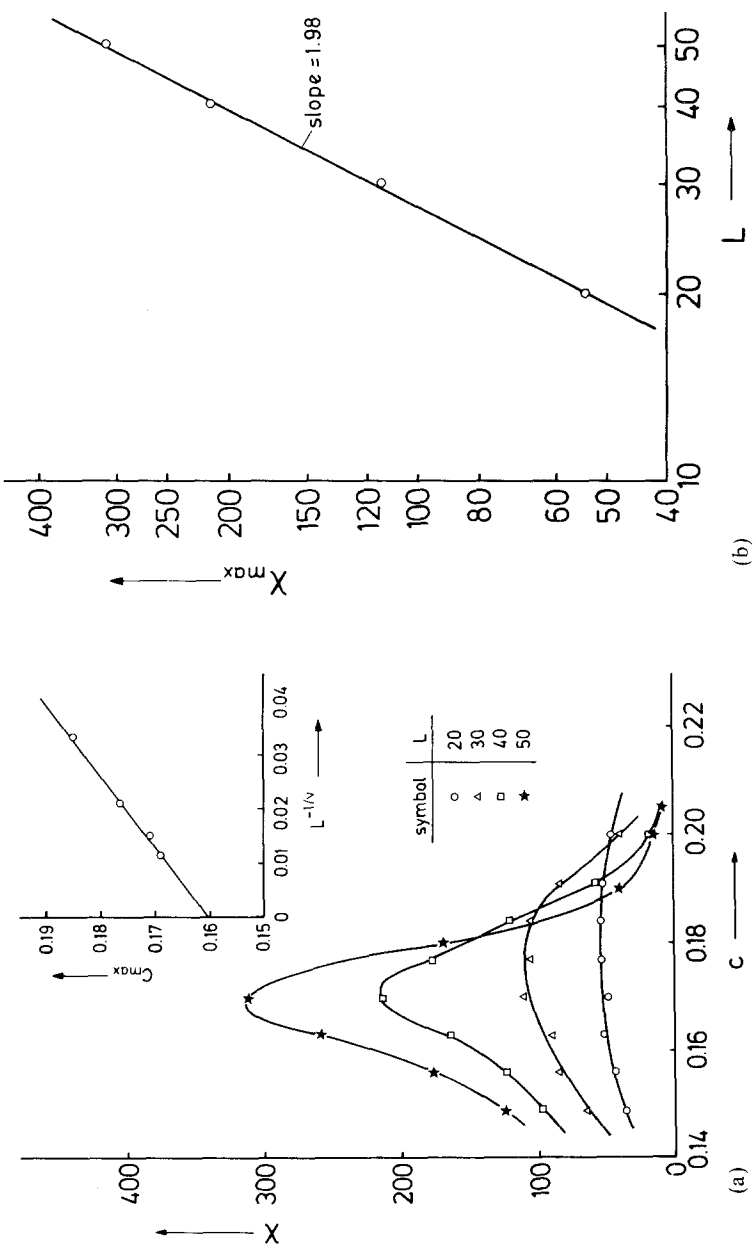

Fig. 7. (a) Percolation susceptibility χ plotted versus concentration c at $T=0$ for several lattice linear dimensions. Inset: a plot of the position $c_{\max}$ of the maximum of χ versus $L^{-1/\nu}$, choosing for ν the value $\nu=0.88$, the correlation length exponent for random percolation.[22–24] (b) Log–log plot of $\chi_{\max}$ versus L. The slope has exactly the value $\gamma/\nu=1.98$ appropriate for random percolation.

3. FINITE-SIZE SCALING ANALYSIS AND DISCUSSION OF CRITICAL BEHAVIOR

It is quite obvious from the "raw data" presented in Figs. 5 and 7 that both P_∞ and χ are strongly affected by finite-size effects, and a careful analysis of these effects is necessary if we wish to analyze the critical exponents of the percolation transition occurring at $c_p^{(\mathrm{corr})}(T, t)$. We hence apply the standard finite-size scaling relations [in this section we abbreviate $c - c_p^{(\mathrm{corr})}(T, t)$ as δc][38–40]

$$P_\infty(L, c) = L^{-\beta/\nu} \bar{P}(\delta c L^{1/\nu}) \tag{2}$$

$$\chi(L, c) = L^{\gamma/\nu} \bar{\chi}(\delta c L^{1/\nu}) \tag{3}$$

where ν is the correlation length exponent, β and γ are the critical exponents of P_∞ and $\chi[P_\infty(L \to \infty) \propto (\delta c)^\beta, \chi(L \to \infty) \propto (\delta c)^{-\gamma}]$, and $\bar{P}$, $\bar{\chi}$ are associate scaling functions.

First we use Eq. (2) to justify the phenomenological intersection method used in Fig. 5 to infer first rough estimates for $c_p^{(\mathrm{corr})}(T, t)$. At fixed L, $P_\infty(L, c)$ is a continuous function near $\delta c = 0$, and hence for small δc we must have

$$\bar{P}(\delta c L^{1/\nu}) \approx \bar{P}(0) + \bar{P}'(0)\, \delta c L^{1/\nu} + \cdots \tag{4}$$

with $\bar{P}'(0) > 0$, since $P_\infty(L, c)$ is an increasing function of c. Now the equation $P_\infty(L, c) = P_\infty(L', c)$ defining an intersection point yields

$$\delta c \approx \frac{L^{-\beta/\nu} - (L')^{-\beta/\nu}}{(L')^{1/\nu - \beta/\nu} - L^{1/\nu - \beta/\nu}} \frac{\bar{P}(0)}{\bar{P}'(0)} \tag{5}$$

Equation (5) shows that $\delta c \to 0$ as $L \to \infty$, i.e., the abscissae of the intersection points do converge toward $c_p^{(\mathrm{corr})}(T, t)$ in Fig. 5. Moreover, one sees that $\delta c > 0$, and hence $c_p^{(\mathrm{corr})}(T, t)$ in general is slightly overestimated by this intersection method. This prediction is consistent with our data: e.g., in Fig. 5e the intersections occur near $c \approx 0.17$, while the extrapolation of the maxima of $\chi(L, c)$ yields $c_p^{(\mathrm{corr})}(0, t) \approx 0.160$ (Fig. 7). Another prediction resulting from Eq. (2) yields for the ordinate of the intersection point a decrease proportional to $L^{-\beta/\nu}$ with increasing L. This prediction also is compatible with the data; see Fig. 5c.

More precise estimates for $c_p^{(\mathrm{corr})}(T, t)$ would result from the intersection method if one would apply it to a quantity the scaling power of which is zero in the finite-size scaling analysis. For standard critical phenomena (e.g., Ising models) a convenient quantity[47] for this purpose is the normalized cumulant of the probability distribution of the order parameter s,

i.e., $\frac{3}{2}U_L \equiv \frac{3}{2} - \langle s^4 \rangle_L / (2\langle s^2 \rangle_L^2)$: It varies between zero and unity, and has a finite nonzero value at criticality. For the percolation problem, an analogous quantity would be the probability $P_s(L, c)$ to have a "spanning cluster" in a finite system of linear dimension L (a "spanning cluster" extends from one boundary of the system throughout the system to the opposite boundary).[48] In the thermodynamic limit, $P_s(\infty, c) = 0$ for $c < c_p^{(\mathrm{corr})}(T, t)$ and $P_s(\infty, c) = 1$ for $c > c_p^{(\mathrm{corr})}(T, t)$ similar to the above quantity $\frac{3}{2}U_\infty$. The finite-size scaling relation for $P_s(L, c)$ simply is

$$P_s(L, c) = \bar{P}_s(\delta c L^{1/\nu}) \tag{6}$$

and hence the equation $P_s(L, c) = P_s(L', c)$ yielding the intersection point implies $\delta c = 0$. In practice, however, $P_s(L, c) = P_s(L', c)$ will also not yield precisely $\delta c = 0$, due to corrections to finite-size scaling. In addition, the statistical effort needed to yield information on $P_s(L, c)$ is much larger than for $P_\infty(L, c)$, and hence $P_s(L, c)$ was not recorded.

In order to get reasonable estimates for $c_p^{(\mathrm{corr})}(T, t)$ from Fig. 5, we proceed as follows: We choose some preliminary estimates for β and ν, and then we plot the abscissa c^* of the intersection point of $P_\infty(L)$ and $P_\infty(L')$ versus the variable

$$[L^{-\beta/\nu} - (L')^{-\beta/\nu}] / [(L')^{1/\nu - \beta/\nu} - L^{1/\nu - \beta/\nu}]$$

Then Eq. (5) implies that all points $c^*(L, L')$ should fall on a straight line; the intersection of this straight line with the ordinate axis is then an improved estimate for $c_p^{(\mathrm{corr})}(T, t)$. Figure 8 shows that this procedure works, but it allows an extrapolation both with the exponents of random percolation ($\beta = 0.45$, $\nu = 0.88$; see Fig. 8a) and with rather different values ($\beta = 0.48$, $\nu = 0.70$; see Fig. 6b). The systematic difference between the estimates for $c_p^{(\mathrm{corr})}(T, t)$ resulting from these extrapolations gives an idea about the accuracy Δc with which we can estimate $c_p^{(\mathrm{corr})}(T, t)$ from our data ($\Delta c \approx 0.005$).

In view of the uncertainty in the precise value of $c_p^{(\mathrm{corr})}(T, t)$, we have tried to analyze our data in terms of Eqs. (2) and (3), treating both the exponent estimates $(1/\nu, \beta/\nu, \gamma/\nu)$ and $c_p^{(\mathrm{corr})}(T, t)$ as fitting parameters. Due to the restricted accuracy of our data for $P_\infty(L, c)$ (Fig. 5) and $\chi(L, c)$ (Fig. 7), it turns out, however, that the fitting procedure does not favor a particular unique choice of parameters β, ν, and $c_p^{(\mathrm{corr})}(T, t)$. Rather, a fit of reasonable quality can be obtained for a broad range of concentrations $c_p^{(\mathrm{corr})}(T, t)$, and the exponent estimates are strongly correlated with the estimate for $c_p^{(\mathrm{corr})}(T, t)$. As a consequence, the accuracy of estimates resulting from this finite-size scaling "data collapsing" procedure is rather uncertain (of course, this is the standard difficulty of this method, as is well known[49]).

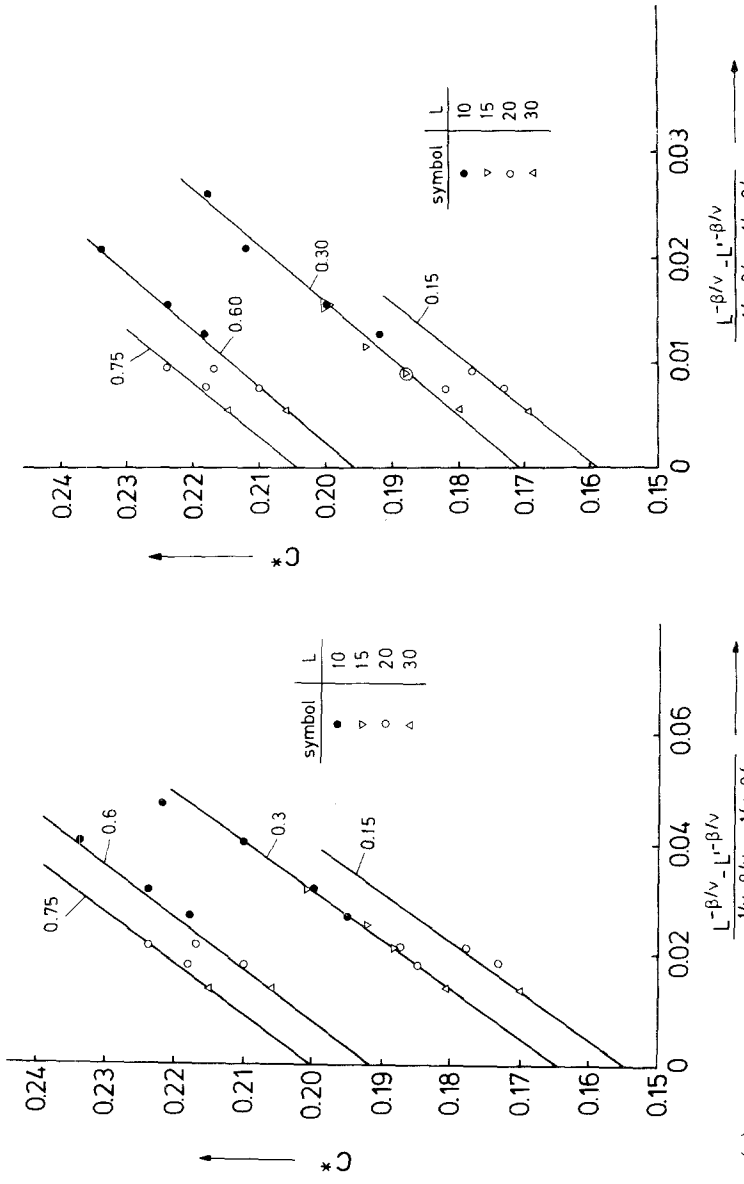

Fig. 8. Plot of the concentration c^* of intersection points $P_\infty(L, c) = P_\infty(L', c)$ for various pairs L, L' as a function of the variable $\{[L^{-\beta/\nu} - (L')^{-\beta/\nu}]/[(L')^{1/\nu-\beta/\nu} - L^{1/\nu-\beta/\nu}]\}$, for various values of T/T_c (parameter of the straight lines). (a) For the random percolation exponents; (b) the choice $\nu = 0.7$, $\beta = 0.48$; in this latter case for $T/T_c = 0.3$ we have used the data for one particular time only ($t = 120$ MCS/site) in order to show that the time averaging does not significantly affect the results.

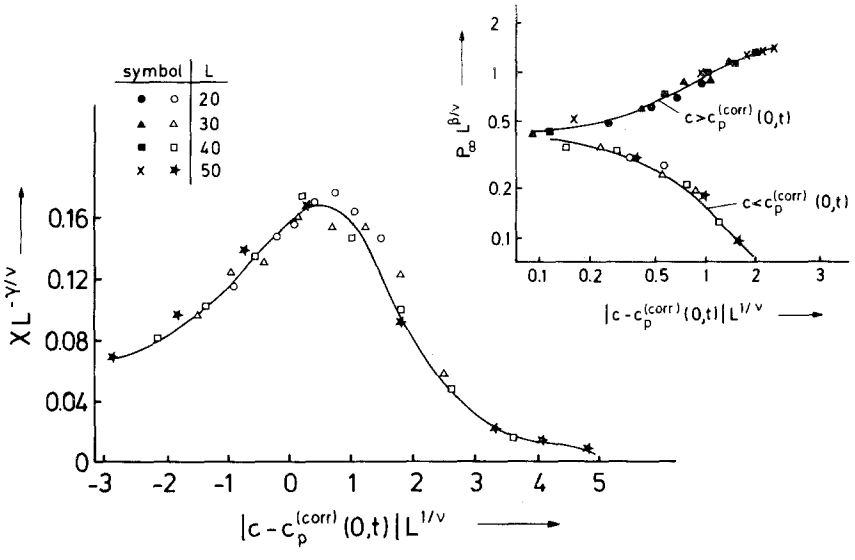

(a)

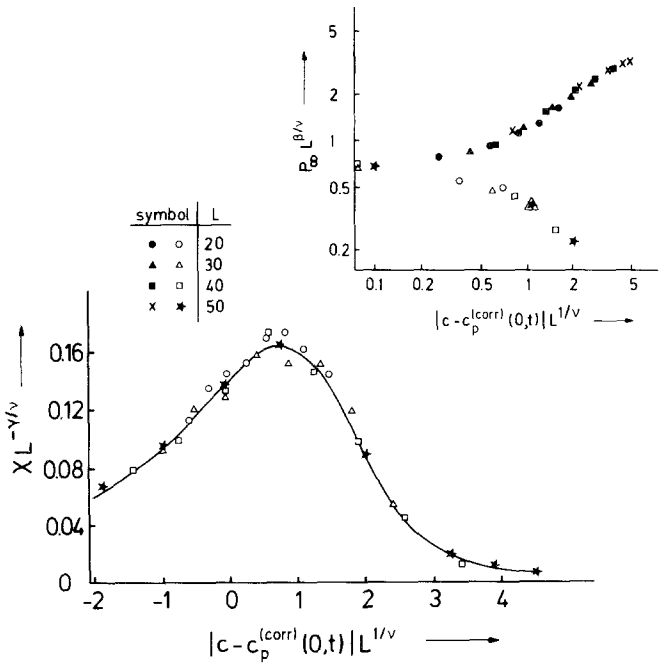

(b)

Fig. 9. Finite-size scaling plots for P_∞ and χ at $T=0$. Both $L^{\beta/\nu}P_\infty(L, c)$ and $L^{-\gamma/\nu}\chi(L, c)$ are plotted versus $\delta c L^{1/\nu}$. The choices $c_p^{(corr)}(0, t) =$ (a) 0.168 and (b) 0.164, with the resulting "best fit" exponents $\beta = 0.12$, $\nu = 0.89$ [from P_∞, case (a)] or $\gamma = 1.50$, $\nu = 0.78$ [from χ, case (a)] or $\beta = 0.28$, $\nu = 0.80$ [from P_∞, case (b)] or $\gamma = 1.56$, $\nu = 0.81$ [from χ, case (b)]. (c) The choice $c_p^{(corr)}(0, t) = 0.160$, with the exponents $\beta = 0.45$, $\gamma = 0.88$, i.e., the known values of the standard random percolation problem[24]. Note that $\gamma/\nu = 1.92$ following from (a) or (b) would also be consistent with the data shown in Fig. 7b within their statistical error.

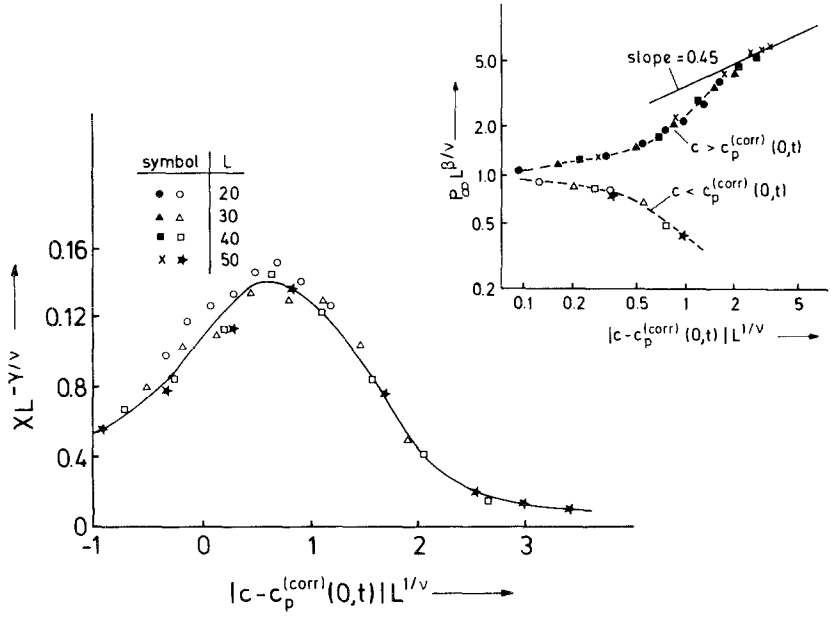

(c)

Fig. 9 (*continued*)

We first analyze the situation for $T=0$. Figure 9 shows three fits for both χ and P_∞. If we choose $c_p^{(\mathrm{corr})}(0, t)=0.168$, which would be closest to the intersection points in Fig. 5c, the estimates for ν resulting from P_∞ and χ are not in full agreement with each other, and the hyperscaling relation $\gamma+2\beta=3\nu$ is strongly violated. Also, for $c_p^{(\mathrm{corr})}(0, t)=0.164$ there is still a distinct violation of the hyperscaling relation, and the fit is obviously not significantly better than in the case shown in Fig. 8c, where we use $c_p^{(\mathrm{corr})}(0, t)=0.160$ (which is a reasonable choice, as shown by the extrapolation in Fig. 7), and the theoretical "best values" for the exponents of the random percolation problem in $d=3$ dimensions, namely[24] $\beta=0.45$, $\gamma=1,74$, $\nu=0.88$. Also, for choices $c_p^{(\mathrm{corr})}(0, r)\approx 0.161$–$0.163$ these random percolation exponents still yield reasonable fits.[44] We conclude that for $T=0$ the percolation transition occurring in these quenching experiments most probably falls in the universality class of standard random percolation.

For $T\neq 0$, however, the situation is not so clear. Irrespective of the choice of $c_p^{(\mathrm{corr})}(T, t)$, we never obtain a "data collapsing" of the curves for $P_\infty(c, L)$ on a single curve with a reasonably small scatter, if we impose the random percolation exponents. Rather, one always sees drastic systematic

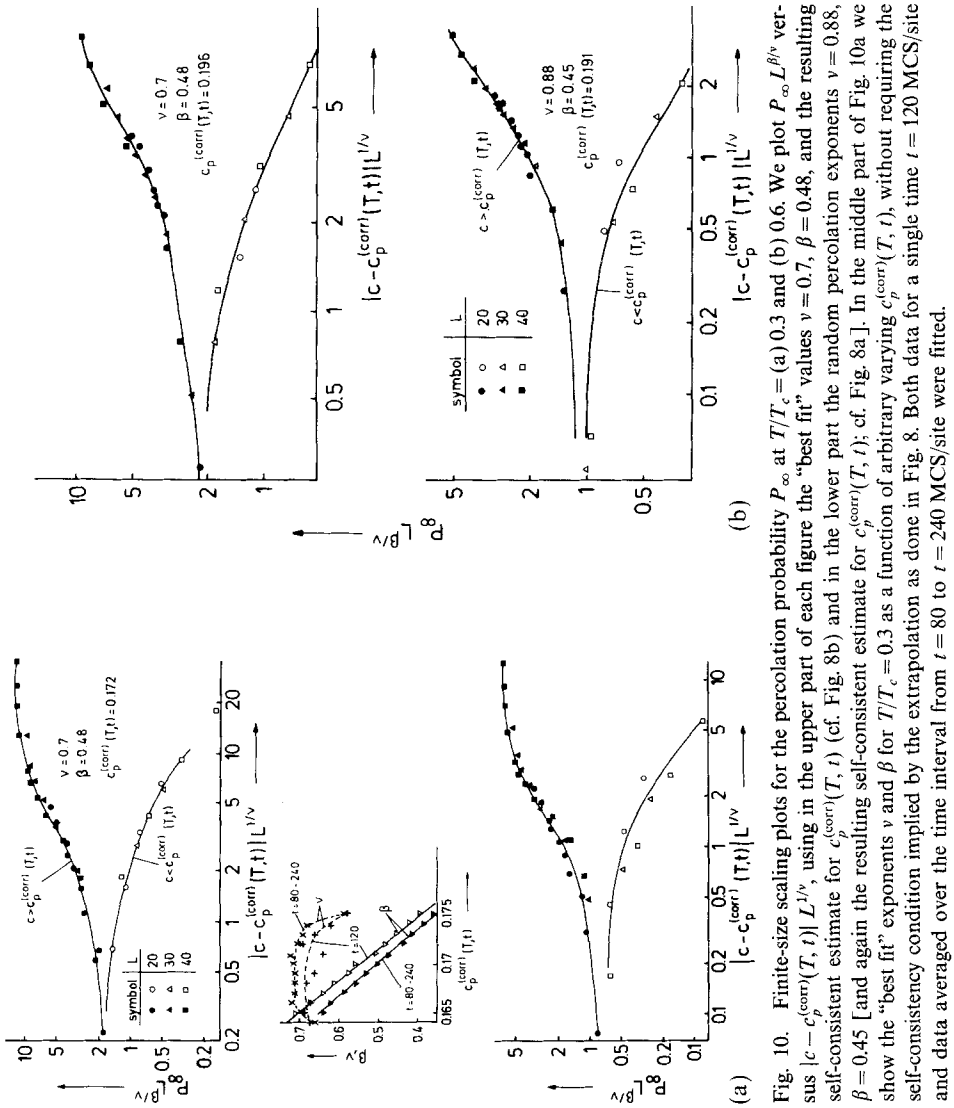

Fig. 10. Finite-size scaling plots for the percolation probability P_∞ at $T/T_c = $ (a) 0.3 and (b) 0.6. We plot $P_\infty L^{\beta/\nu}$ versus $|c - c_p^{(corr)}(T,t)| L^{1/\nu}$, using in the upper part of each figure the "best fit" values $\nu = 0.7$, $\beta = 0.48$, and the resulting self-consistent estimate for $c_p^{(corr)}(T,t)$ (cf. Fig. 8b) and in the lower part the random percolation exponents $\nu = 0.88$, $\beta = 0.45$ [and again the resulting self-consistent estimate for $c_p^{(corr)}(T,t)$; cf. Fig. 8a]. In the middle part of Fig. 10a we show the "best fit" exponents ν and β for $T/T_c = 0.3$ as a function of arbitrary varying $c_p^{(corr)}(T,t)$, without requiring the self-consistency condition implied by the extrapolation as done in Fig. 8. Both data for a single time $t = 120$ MCS/site and data averaged over the time interval from $t = 80$ to $t = 240$ MCS/site were fitted.

deviations, as shown in the examples presented in Fig. 10. On the other hand, now the "best fit" exponents are fairly independent of temperature, and also the estimate for ν is distinctly smaller than the random percolation value. Note that while β is strongly dependent on the choice of $c_p^{(\mathrm{corr})}(T, t)$, ν varies much less. Varying $c_p^{(\mathrm{corr})}(T=0.3, t)$ from 0.177 to 0.187, we find that only values ν in between 0.55 and 0.71 occur. Varying $c_p^{(\mathrm{corr})}(T=0.6, t)$ from 0.199 to 0.209, we find only values of ν between 0.50 and 0.68. Also, Fig. 8 shows relatively little variation of the fitted ν with $c_p^{(\mathrm{corr})}(0, t)$. This result could mean that the critical behavior along the percolation transition line $c_p^{(\mathrm{corr})}(T, t)$ for $T>0$ belongs to a different universality class than that of the transition at $T=0$, which we believe is simply random percolation, though with a critical concentration only about one-half as large as in the random site percolation problem. Such a conclusion, if correct, would be rather surprising, since the percolation transition along the whole line $c_p^{(\mathrm{corr})}(T)$ in the one-phase region belongs to the universality class of simple random percolation again.

In order to study this problem further, we have also studied the cluster size distribution function $n_l(t)$ at the critical concentration $c=c_p^{(\mathrm{corr})}(T, t)$; see Fig. 11. Since our lattices are rather small and the effective critical concentration is shifted to larger values for these small lattice sizes L, we have chosen those effective values rather than the values extrapolated to $L \to \infty$ in Fig. 8. It is seen that the data are reasonably consistent with the expected power law variation[22]

$$n_l(t) \propto l^{-\tau}, \qquad \tau = 2 + 1/\delta \tag{7}$$

In all cases we find an exponent $\tau > 2$, as it should be, and again at $T=0$ it is nicely consistent with the theoretical value of random percolation $[1/\delta = \beta/(\gamma+\delta) \approx 0.21]$, while for $T>0$, τ seems to be somewhat smaller, implying a smaller value of $1/\delta$, consistent with the estimate $1/\delta \approx 0.16$ following from the estimates for β and γ quoted above. However, the statistical errors of τ always are of the order of 0.05 at least, and there may be an additional systematic error due to the inaccuracy in the choice of $c_p^{(\mathrm{corr})}(T, t)$. From the data in Fig. 10 we cannot rule out that one observes simple random percolation at all temperatures.

Obviously, the accuracy of our study of the critical behavior of the percolation transition in phase separation is by far less than the accuracy that now is standard in the study of the ordinary percolation problem.[24,48–50] Of course, this must be expected. In one MCS/site one generates a new and statistically independent configuration of the lattice for the ordinary site percolation problem, while in the present problem we have to let the system evolve of the order of 100 MCS/site to generate a new configuration.

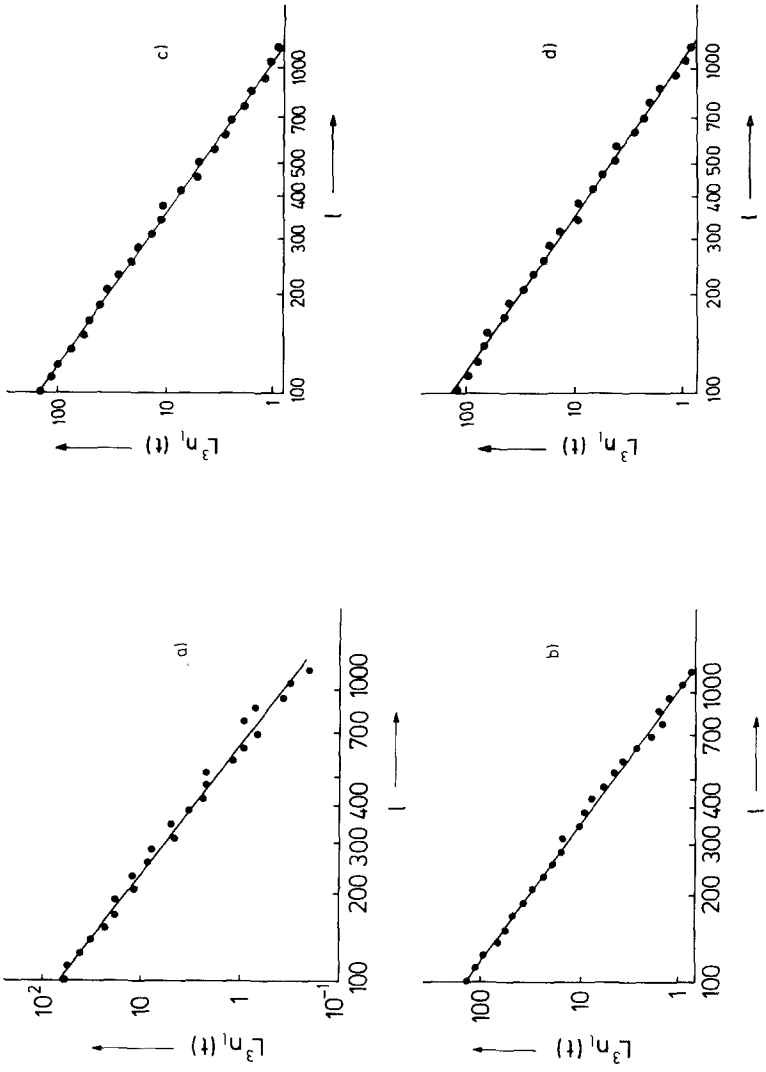

Fig. 11. Log–log plots of the cluster size distribution $n_l(t)$ versus cluster size l at the critical concentration. All data refer to a lattice size $L = 40$; in case (a), which refers to $T = 0$, the time average was taken from $t = 85$ to $t = 100$ MCS/site, while in all other cases it was taken from $t = 80$ to $t = 240$ MCS/site. (a) $T = 0$, $c_p^{(\mathrm{corr})}(0, t) = 0.160$, and the straight line indicates an exponent $\tau = 2.24$; (b) $T = 0.15T_c$, $c^{(\mathrm{corr})}(T, t) = 0.171$, $\tau = 2.15$; (c) $T = 0.3T_c$, $c_p^{(\mathrm{corr})}(T, t) = 0.182$, $\tau = 2.14$; (d) $T = 0.6T_c$, $c_p^{(\mathrm{corr})}(T, t) = 0.204$, $\tau = 2.07$.

4. DISCUSSION

The main result of this paper is contained in Fig. 6, where it is shown that a percolation transition can be located throughout the two-phase region of an Ising lattice gas model occurring during the intermediate stages of phase separation (t being of the order of 100 MCS/spin). At $T=0$, we obtain evidence that the percolation transition belongs to the universality class of simple random percolation, although the critical concentration is reduced by about a factor of two [$c_p^{(\mathrm{corr})} \approx 0.31$, $c_p^{(\mathrm{corr})}(T=0, t) \approx 0.16$]. Although a reduction of the critical concentration in comparison with $c_p^{(\mathrm{corr})}$ is expected, since the "monomers" are removed from the system during the process and attached to the larger clusters (Fig. 4), the large amount of this reduction was unexpected [note that for $c = c_p^{(\mathrm{corr})}$ only about 12% of the occupied sites belong to monomers]. For $T > 0$, the critical behavior seems to be less compatible with that of random percolation, and indicates different exponents, which would imply that the transient dynamic percolation during phase separation belongs to a new universality class. This finding is rather unexpected, since the dynamic structure factor $S(\mathbf{k}, t)$ exhibits no significant correlations at large distances during the early and intermediate stages of phase separation. Correlations are seen in $S(\mathbf{k}, t)$ only from small distances up to the characteristic length scale $l(t)$, and on length scales $L \gg l(t)$ the configuration is still rather random. Of course, it may be that the intrinsic instability of the system influences the diffusion process on large length scales in such a way that the cluster statistics is strongly affected even for cluster sizes much larger than $l(t)$. From the studies of *irreversible* growth phenomena such as diffusion-limited aggregation or cluster–cluster aggregation,[4] one knows that the existing irregular clusters have a strong effect on the probability distribution for the diffusion of the surrounding objects. Since the percolation cluster in our case also appears as a result of a specific growth phenomenon, it is conceivable that it belongs to a new universality class.

What are the consequences of the percolation transition at $c_p^{(\mathrm{corr})}(T, t)$ for our understanding of phase separation dynamics? It is not obvious that one can see any singular behavior in the dynamic structure factor $S(\mathbf{k}, t)$. After all, the percolation transition at $c_p^{(\mathrm{corr})}(T)$ in the one-phase region is irrelevant for the static structure function $S_T(\mathbf{k})$, which is singular at the critical point only. It is well known that "physical clusters"[29,30] rather than geometrical clusters show up in the physical correlation functions. At low temperatures physical and geometrical clusters do become identical, however. Thus, it is reasonable to expect that if one studies the percolation of "physical clusters" instead of geometrical clusters during phase

[4] For a thorough recent review of growth phenomena see Ref. 51.

separation, one will find a line of percolation transitions similar to Fig. 6, starting at $T=0$ at the same point $c_p^{(\mathrm{corr})}(0, t) \approx 0.16$, but at higher temperatures it will deviate distinctly from $c_p^{(\mathrm{corr})}(0, t)$ and bend over to higher concentrations, to end at the critical point $T=T_c$, $c=c_{\mathrm{crit}}=1/2$, similar to the dash-dotted curve in Fig. 1 describing the percolation transition in the coarse-grained structure of the late stages. Neither of these percolation phenomena is taken into account in current theoretical descriptions of phase separation kinetics. In fact, much recent activity has been directed toward an extension of the Lifshitz–Slyozov[52] cluster-evaporation and condensation mechanism to higher concentrations.[53–64,37] All these treatments, as well as work considering the droplet diffusion and coagulation mechanism,[37] treat the clusters as essentially compact, spherical objects. In contrast, our work shows that the usefulness of these approaches probably is restricted to concentrations distinctly smaller than $c_p^{(\mathrm{corr})}(T, t)$. We have an infinite percolating net, and coarsening proceeds by the breakoff of atoms from dangling ends or other small-scale structure of the net. These atoms diffuse around in the matrix and get reattached to the net in such a way that thin links in the net either get thickened or "evaporate." Right at $c_p^{(\mathrm{corr})}(T, t)$, we still have very large but finite separated clusters, described by the distribution (7), but they are not compact objects, but rather fractals.[33] Their fractal dimensionality d_f can be expressed in terms of the exponents of the percolation transition in the standard way[24] as

$$d_f = d - \beta/\gamma \approx 2.49 \tag{8}$$

where we have used the exponents appropriate for random percolation [if the transition at $c_p^{(\mathrm{corr})}(T, t)$ belongs to a different universality class with $\beta \approx 0.48$, $\gamma = 0.70$, $d_f \approx 2.3$, which implies that the clusters would be slightly less compact].

Various mechanisms of cluster growth and coarsening considered in Refs. 37 and 51–64 assume compact (essentially spherical) droplets. However, the large but finite clusters that occur for concentrations c slightly below $c_p^{(\mathrm{corr})}(T, t)$ [which are described by the cluster size distribution $n_l(t) \propto l^{-\tau}$ for $l \to \infty$ at $c = c_p^{(\mathrm{corr})}(T, t)$] are not at all compact, but rather ramified objects. This fractal structure should have a pronounced effect on the rates of the various cluster growth mechanisms; e.g., a standard assumption is that the number of atoms evaporating from the surface of a cluster containing l sites per unit time is a rate constant Γ times the surface area of the cluster. For a compact d-dimensional cluster the surface area S_l is proportional to $l^{1-1/d}$, and this power law $S_l \propto l^{1-1/d}$ is used explicitly both in the derivation of the Lifshitz–Slyozov[51,35] law $l(t) \propto t^{d/3}$ and in the derivation of the growth law $l(t) \propto t^{d/(d+3)}$ resulting from cluster

diffusion and coagulation[35,37] when one assumes that the cluster diffusion is due to atoms that evaporate and reimpinge on the same cluster. A single event of this type produces a shift of the cluster center of gravity of order l^{-1}. Then the cluster diffusion constant is $D_l \propto S_l l^{-2} \propto l^{-1-1/d}$. Assuming that two clusters of about the same size l can coalesce when they have diffused a distance of their own size l, which needs a time Δt given by $l^{2/d} = D_l \Delta t$, one obtains

$$dl/dt \approx \Delta l/\Delta t \approx l/(l^{2/d}/D_l) \propto l^{-3/d}, \qquad l(t) \propto t^{d/(d+3)}$$

as quoted above. Assuming now fractal instead of compact clusters, we have $S_l \propto l^{\zeta}$ with $\zeta > 1 - 1/d$, and $D_l \propto l^{\zeta-2}$. Then the same reasoning as above would yield instead

$$dl/dt \approx l/(l^{2/d_f}/D_l) \propto l^{\zeta-1-2/d_f}$$

and the growth law would become $l(t) \propto t^{1/[2-\zeta+2/d_f]}$. The fractal structure in this case would be reflected in a nontrivial value of the growth exponent relating the typical domain size $l(t)$ to the time t.

Binder and Kalos[37] pointed out that at temperatures not too low the dominating mechanism of cluster diffusion is effected by random evaporation and condensation events of atoms the typical distance of which is of the order of the cluster linear dimension itself. Then

$$D_l \propto S_l (l^{-1+1/d_f})^2 \propto l^{\zeta-2+2/d_f} \tag{9}$$

and since $d_f \approx 2$ for $d = 2$ and $\zeta = 1$ for rather ramified objects, one would obtain a cluster diffusion constant that does not decrease with cluster size, i.e., a rapid diffusion of clusters would result. The physical consequences of this rather rapid motion of the clusters near $c_p^{(\mathrm{corr})}(T, t)$, as well as the accompanying rapid rearrangements of their shapes, need to be elucidated.

An alternative growth mechanism of the fractal clusters might be a "filling in" of the domains, which then initially would compactify. This mechanism was observed in Ref. 68 in a medium-range model with nonconserved order parameter. It is not clear to what extent this mechanism is effective in the present model with conserved concentration, where monomers would have to diffuse to the center of the domains from the outside in order to compactify. This diffusion to the center will probably be screened out, similar to what happens during cluster growth in diffusion-limited aggregation.

Another property of the clusters becomes crucial in the limit $T \to 0$. Then predominantly only particular atoms can be broken off a cluster by thermal fluctuations, namely those atoms that in "dangling ends" are

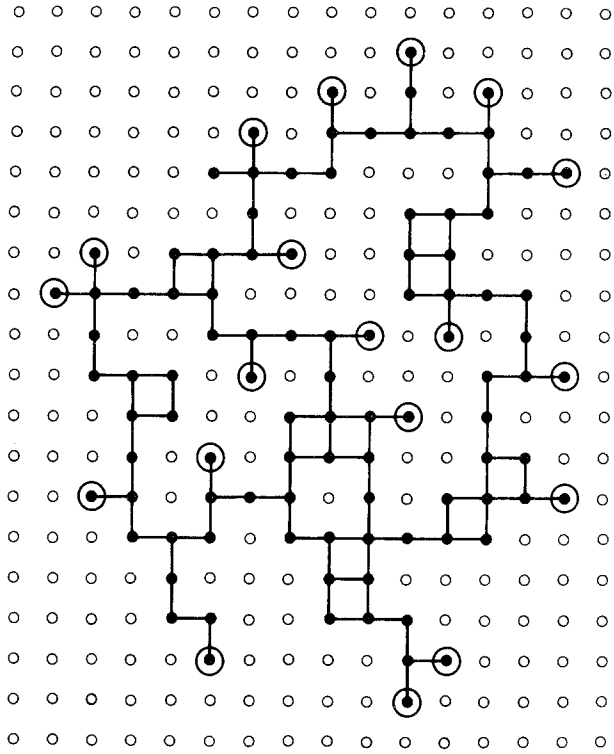

Fig. 12. Schematic picture of a fractal cluster as it occurs near the percolation threshold $c_0^{(\mathrm{corr})}(T \to 0, t)$ in phase separation dynamics. The atoms in dangling ends are encircled; predominantly those atoms contribute to the further time evolution of the system.

bound to a single other atom of the cluster (Fig. 12). For the number $n_d(l)$ of atoms in dangling ends of an l-cluster we again expect a power law

$$n_d(l) \propto l^{\theta} \tag{10}$$

but the exponent θ is unknown. At low enough temperatures, it may be appropriate to replace S_l by $n_d(l)$ in the above formulas for the cluster diffusivity and in the consideration of the Lifshitz–Slyozov mechanism. Another rather intriguing aspect of our results is that the finding $c_p^{(\mathrm{corr})}(0, t) \approx 0.16$ happens to agree with the so-called critical volume fraction $\phi_c = 0.16$,[65,66] which is the percolation treshold when spheres are randomly placed in the continuum. It has been suggested [32] that there exists a critical volume fraction of the coexisting phases,

$$\phi_{\mathrm{crit}} = \frac{c - c_{\mathrm{coex}}^{(1)}}{c_{\mathrm{coex}}^{c} - c_{\mathrm{coex}}^{(1)}}$$

where the macroscopic structure of phase-separated domains of the two phases having the concentrations $c_{\text{coex}}^{(1)}$ and $c_{\text{coex}}^{(2)}$ percolate (the inner dash-dotted curve in Fig. 1). It is tempting to speculate that ϕ_{crit} is the same as ϕ_c; this would imply that the two dash-dotted curves in Fig. 1, describing percolation thresholds for intermediate and for late stages, end at $T=0$ in the same point.

We are fully aware that this whole section is very speculative, and poses many questions rather than yielding definitive results. But we feel that understanding the dynamics of coarsening of percolating structures is crucial for making progress in the understanding of phase separation kinetics, and hope that the present work will be a stimulating starting point for further work along these lines.

ACKNOWLEDGMENT

This work was partially supported by the Deutsche Forschungsgemeinschaft, SFB 41.

REFERENCES

1. J. D. Gunton, M. San Miguel, and P. S. Sahni, in *Phase Transitions and Critical Phenomena*, Vol. 8, C. Domb and J. L. Lebowitz, eds. (Academic Press, New York, 1983), p. 267.
2. K. Binder, in *Condensed Matter Research Using Neutrons*, S. W. Lovesey and R. Scherm, eds. (Plenum Press, New York, 1984), p. 1.
3. K. Binder, *Rep. Progr. Phys.* **50**:783 (1987).
4. A. C. Zettlemoyer (ed.), *Nucleation* (Dekker, New York, 1969).
5. F. F. Abraham, *Homogeneous Nucleation Theory* (Academic Press, New York, 1974).
6. K. Binder and D. Stauffer, *Adv. Phys.* **25**:343 (1976).
7. J. W. Cahn, *Acta Met.* **9**:795 (1961).
8. J. W. Cahn, *Trans. Met. Soc. AIME* **242**:166 (1968).
9. J. S. Langer, *Ann. Phys.* **65**:53 (1971); *Acta Met.* **21**:1649 (1973); J. S. Langer, M. Baron, and H.-D. Miller, *Phys. Rev. A* **11**:1417 (1975).
10. J. W. Cahn and J. E. Hilliard, *J. Chem. Phys.* **31**:688 (1959).
11. J. D. Gunton and M. C. Yalabik, *Phys. Rev. B* **18**:6199 (1978); G. Dee, J. D. Gunton, and K. Kawasaki, *J. Stat. Phys.* **24**:87 (1981).
12. W. Klein, *Phys. Rev. Lett.* **47**:1569 (1981).
13. W. Klein and C. Unger, *Phys. Rev. B* **28**:445 (1983); C. Unger and W. Klein, *Phys. Rev. B* **29**:2698 (1984).
14. K. Binder, *Phys. Rev. A* **29**:34 (1984).
15. R. B. Griffiths, C. Y. Weng, and J. S. Langer, *Phys. Rev.* **149**:301 (1966).
16. O. Penrose and J. L. Lebowitz, *J. Stat. Phys.* **3**:211 (1971).
17. K. Binder, *Phys. Rev. B* **8**:3423 (1973).
18. D. W. Heermann, W. Klein, and D. Stauffer, *Phys. Rev. Lett.* **49**:1262 (1982).
19. D. W. Heermann, *Phys. Rev. Lett.* **52**:1126 (1984); *Z. Phys. B* **61**:311 (1985).
20. K. Kaski, K. Binder, and J. D. Gunton, *Phys. Rev. B* **29**:3996 (1984).

21. K. Binder, C. Billotet, and P. Minold, *Z. Phys. B* **30**:1183 (1978).
22. D. Stauffer, *Phys. Rep.* **54**:1 (1979).
23. J. W. Essam, *Rep. Progr. Phys.* **43**:843 (1980).
24. D. Stauffer, *An Introduction to Percolation Theory* (Taylor and Francis, London, 1985).
25. A. Coniglio, *J. Phys. A* **8**:1773 (1975); A. Coniglio, F. Peruggi, C. Nappi, and L. Russo, *J. Phys. A* **10**:205 (1977).
26. H. Müller-Krumbhaar, *Phys. Lett.* **50A**:27 (1974).
27. D. W. Heermann and D. Stauffer, *Z. Phys.* **44**:339 (1981).
28. D. W. Heermann, *Z. Phys. B* **55**:309 (1984).
29. A. Coniglio and W. Klein, *J. Phys. A* **13**:2775 (1980).
30. C.-K. Hu, *Phys. Rev. B* **29**:5103 (1984).
31. D. W. Heermann and W. Klein, *Phys. Rev. B* **27**:1732 (1983).
32. K. Binder, *Solid State Commun.* **34**:191 (1980).
33. B. B. Mandelbrot, *Fractals: Form, Chance, and Dimension* (Freeman, San Francisco, 1977); *The Fractal Geometry of Nature* (Freeman, San Francisco, 1982).
34. M. Schöbinger, S. W. Koch, and F. F. Abraham, *J. Stat. Phys.* **42**:1071 (1986); S. W. Koch, in *Advances on Phase Transitions and Disorder Phenomena*, G. Busiello, L. De Cesare, F. Mancini, and M. Marinaro, eds. (World Scientific, Singapore, 1987), p. 72; R. C. Desai and A. R. Denton, in *On Growth and Form*, (H. E. Stanley and N. Ostrowsky, eds. (Martinus Nishoff, Boston, 1986), p. 237.
35. K. Binder and D. W. Heermann, in *Scaling Phenomena in Disordered Systems*, R. Pynn and A. Skjeltorp, eds. (Plenum Press, New York, 1985), p. 207.
36. H. Furukawa, *Adv. Phys.* **34**:703 (1986).
37. K. Binder, *Phys. Rev. B* **15**:4424 (1977); K. Binder and D. Stauffer, *Phys. Rev. Lett.* **33**:1006 (1974); K. Binder and M. H. Kalos, *J. Stat. Phys.* **22**:3363 (1980).
38. M. N. Barber, in *Phase Transitions and Critical Phenomena*, Vol. 8, C. Domb and J. L. Lebowitz, eds. (Academic Press, New York, 1983), p. 146; M. E. Fisher and M. N. Barber, *Phys. Rev. Lett.* **28**:1516 (1972).
39. K. Binder, *Ferroelectrics* **73**:43 (1987); see also K. Binder, *Z. Phys. B* **43**:119 (1981).
40. A. Margolina and H. J. Herrmann, *Phys. Lett.* **104A**:295 (1984).
41. K. Kawasaki, in *Phase Transitions and Critical Phenomena*, Vol. 2, C. Domb and M. S. Green, eds. (Academic Press, New York, 1972), p. 443.
42. K. Binder and M. H. Kalos, in *Monte Carlo Methods in Statistical Physics*, K. Binder, ed. (Springer, Berlin, 1979), p. 225.
43. D. W. Heermann, *Introduction to Computer Simulation Methods in Theoretical Physics* (Springer, Berlin, 1986).
44. S. Hayward, Diplomarbeit, Johannes-Gutenberg-Universität, Mainz (1987), unpublished.
45. D. W. Heermann, Thesis, Boston University (1983), unpublished.
46. P. A. Meakin and S. Reich, *Phys. Lett.* **92A**:247 (1982); A. Levy, S. Reich, and P. Meakin, *Phys. Lett.* **87A**:248 (1982); R. G. Palmer and H. L. Frisch, *J. Stat. Phys.* **38**:867 (1985).
47. K. Binder, *Z. Phys. B* **43**:119 (1981).
48. S. Kirpatrick, in *Ill-Condensed Matter*, R. Balian, R. Maynard, and G. Toulouse, eds. (North-Holland, Amsterdam, 1979), p. 321.
49. K. Binder and D. Stauffer, in *Applications of the Monte Carlo Method in Statistical Physics*, K. Binder, ed. Springer, Berlin, 1984), p. 1.
50. K. Binder and D. Stauffer, in *Applications of the Monte Carlo Method in Statistical Physics*, K. Binder, ed. (Springer, Berlin, 1984), Chapter 8.
51. H. J. Herrmann, *Phys. Rep.* **136**:154 (1986).
52. I. M. Lifshitz and V. V. Slyozov, *J. Phys. Chem. Solids* **19**:35 (1961).
53. J. J. Weins and J. W. Cahn, in *Sintering and Related Phenomena*, G. C. Kuczynski, ed. (Plenum Press, New York, 1973), p. 151.

54. K. Kawasaki and T. Ohta, *Physica* **118A**:175 (1983); M. Tokuyama and K. Kawasaki, *Physica* **123A**:386 (1984).
55. T. Ohta, *Ann. Phys.* **158**:31 (1984); *Progr. Theor. Phys.* **71**:1409 (1984).
56. J. A. Marqusee and J. Ross, *J. Chem. Phys.* **80**:536 (1984).
57. H. Tomita, *Progr. Theor. Phys.* **71**:1405 (1984); **72**:656 (1984).
58. M. Tokuyama, Y. Enomoto, and K. Kawasaki, preprints.
59. H. Furukawa, *Phys. Rev. A* **29**:2160 (1984); *A* **30**:1052 (1984); *Physica A* **123**:497 (1984); *Progr. Theor. Phys.* **73**:586 (1985).
60. P. W. Voorhees, *J. Stat. Phys.* **38**:231 (1985); P. W. Voorhees and M. E. Glicksman, *Acta Met.* **32**:2001, 2013 (1984).
61. J. S. Langer and A. J. Schwartz, *Phys. Rev. A* **21**:948 (1980); R. Kampmann and R. Wagner, in *Decomposition of Alloys: The Early Stages*, P. Haasen, V. Gerold, R. Wagner, and M. F. Ashby, eds. (Pergamon Press, 1984), p. 143.
62. P. W. Voorhees and M. E. Glicksman, *Met. Trans. A* **15**:1081 (1984); see also W. J. Beenakker and J. Ross, *J. Chem. Phys.* **83**:4710 (1985).
63. C. W. J. Beenakker, preprint; C. W. J. Beenakker and J. Ross, preprint.
64. M. P. Marder, preprint.
65. H. Scher and R. Zallen, *J. Chem. Phys.* **53**:3759 (1970).
66. I. Webman, J. Jortner, and M. H. Cohen, *Phys. Rev. B* **14**:4737 (1976).
67. G. S. Grest and D. J. Srolovitz, *Phys. Rev. B* **30**:5150 (1984).
68. D. W. Heermann and W. Klein, *Phys. Rev. Lett.* **50**:1062 (1983).